Structure, crystal fields, magnetic interactions, and heavy-fermion behavior in $(Ce_{1-x}La_x)_3Al$

Y. Y. Chen and Y. D. Yao
Institute of Physics, Academia Sinica, Taipei, Taiwan, Republic of China

B. C. Hu and C. H. Jang
Department of Physics, Fu Jen University, Taiwan, Republic of China

J. M. Lawrence
Department of Physics, University of California, Irvine, California 92717

H. Huang and W. H. Li
Department of Physics, National Central University, Taiwan, Republic of China

(Received 6 May 1996)

We report measurements of the resistivity ρ, susceptibility χ, and specific heat C of the alloys $(Ce_{1-x}La_x)_3Al$. At room temperature these form in the hexagonal Ni_3Sn structure (α-Ce_3Al); at low temperatures a structural transition to a monoclinic phase occurs for $0 \leqslant x \leqslant 0.3$ (γ-Ce_3Al); and a transition with a similar feature in the resistivity occurs for $0.75 < x \leqslant 1$ (γ-La_3Al). Crystal fields have strong effects on these measurements: analysis of the specific heat suggests that for Ce_3Al two excited doublets occur at temperatures $T_{1cf} \approx 75$ K and $T_{2cf} \approx 130$ K above the ground-state doublet, and that these splittings decrease significantly on alloying; this causes a similar decrease in the Curie-Weiss temperature θ_h obtained from the high-temperature susceptibility $\chi = C/(T + \theta_h)$. The derivative $d\rho/dT$ of the low-temperature resistivity is negative over a range of temperature for all x ($0 \leqslant x < 1$), which is a characteristic sign of heavy-fermion (Kondo) behavior; various measures of the Kondo temperature T_K, taken from the analysis of ρ, χ, and C, consistently suggest that T_K decreases by an order of magnitude on alloying, from ≈ 10 K for small x to ≈ 1 K for large x. Fits to the low-temperature specific heat which include a lattice contribution, a crystal-field contribution, and an $S = 1/2$ Kondo contribution describe the data well for $x = 0.95$; but for $0.3 \leqslant x \leqslant 0.82$ the specific heat peak is larger and narrower than predicted by Kondo theory and a peak occurs in the resistivity, suggesting that coherence due to magnetic correlations plays a role for these concentrations. For the monoclinic phase, peaks in ρ, χ, and C indicate antiferromagnetic order, where the Néel temperature decreases with x from its value $T_N = 2.5$ K for $x = 0$. The specific heat is linear at the lowest temperatures, even in the antiferromagnetic phase, which suggests that the magnetic order coexists with Kondo behavior. [S0163-1829(97)02309-6]

I. INTRODUCTION

Heavy-fermion behavior is observed[1] in the systems Ce_3X (X=In, Sn, Al). For Ce_3Al, the room-temperature phase (α-Ce_3Al) is hexagonal (Ni_3Sn) but a structural transition occurs at $T_s = 110$ K.[1,2] An initial study[3] using conventional x-ray diffraction found that the low-temperature state also has the Ni_3Sn structure. However, Rietveld refinement of the structure using high-resolution diffraction data from a spallation neutron source found the low-temperature phase to be monoclinic;[4] the monoclinic structure was confirmed[5] using neutron data from a triple-axis spectrometer. In this γ-Ce_3Al phase antiferromagnetic order occurs at $T_N = 2.5$ K.[1–3] For $T > T_N$ the low-temperature resistivity exhibits a negative derivative $d\rho/dT$; this Kondo effect establishes that the magnetic order occurs at a temperature where heavy-fermion processes are active in removing the spin entropy. A common way to study the resulting interplay between magnetic order and heavy-fermion behavior is through substitution of nonmagnetic La for Ce. Older studies[6,7] of the resistivity $\rho(T)$ and susceptibility $\chi(T)$ from 2–300 K in the system $(Ce_{1-x}La_x)_3Al$ explored a limited range of alloy concentration ($x < 0.3$); these show that the low-temperature structural transition vanishes for $x > 0.2$; i.e., $T_s(x) \rightarrow 0$ for $0.2 < x < 0.3$. A study[8] of the specific heat $C(T)$ for $0 \leqslant x \leqslant 0.67$ and 1.2 K $< T <$ 300 K suggests that the Néel temperature T_N initially decreases with x, but then saturates to a value of order 1.5 K.

In this paper we report a more thorough study, wherein ρ, χ, and C are all measured for a series of alloys spanning the range $0 \leqslant x \leqslant 1$. The measurements of $C(T)$ and (for select compounds) of $\rho(T)$ were extended to a lower temperature (0.5 K) than in the previous studies. In the analysis and discussion we focus on the interplay between structure, crystal fields, magnetic interactions, and the Kondo effect.

II. EXPERIMENTAL DETAILS

Polycrystalline samples of $(Ce_{1-x}La_x)_3Al$ for $x = 0$, 0.06, 0.12, 0.2, 0.25, 0.3, 0.7, 0.82, 0.95, and 1 were prepared by arc melting the constituent elements in an argon atmosphere. High-purity Ce(99.99%), Al(99.9999%), and La(99.9%) were obtained from the Johnson Matthey Company. To avoid oxidation the cerium was prepared in a pure nitrogen atmosphere. The as-cast samples were then annealed at

 © 1997 The American Physical Society

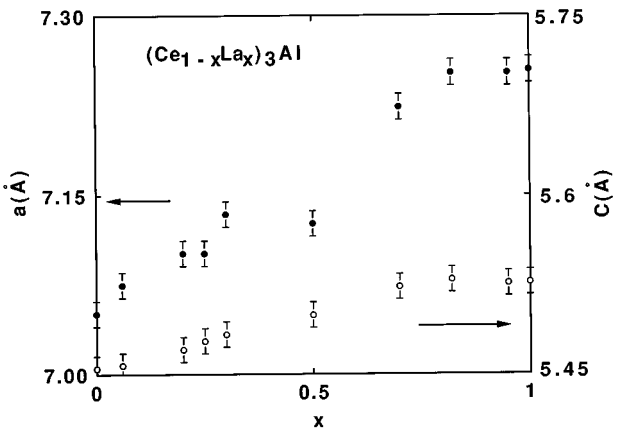

FIG. 1. The room-temperature lattice parameters for $(Ce_{1-x}La_x)_3Al$ for different concentrations x.

200 °C for 10 days to eliminate any residual high-temperature cubic β-Ce_3Al phase. X-ray diffraction was performed at room temperature for all x on polished bulk specimens using a rotating anode diffractometer manufactured by Materials Analysis and Characterization. These studies demonstrate that at room temperature the alloys have the Ni_3Sn structure for all x with no evidence for second phases within the detection limits (a few percent) of the instrument. The lattice constants vary smoothly with x (Fig. 1). For Ce_3Al diffraction measurements on these polished specimens were also measured at low temperature; for both Ce_3Al and La_3Al additional studies (discussed below) at room temperature and low temperature were performed on annealed powders formed by filing the bulk ingots. The specific heat was measured in the range 0.4–60 K using a thermal-relaxation microcalorimeter[9] and samples of approximately 2×2 mm^2 cross section and 0.2 mm thickness. Measurements of the magnetic susceptibility for $1.8<T<300$ K were implemented in a superconducting quantum interference device which was calibrated with a palladium standard prior to the measurements. Resistivity measurements for $1.2<T<300$ K were performed by the standard four-probe method on samples with a rectilinear geometry; for $x=0.3$, 0.7 the lower limit on T was 0.3 K; for $x=0.3$, 0.7 the lower limit on T was 0.3 K. To establish reproducibility, measurements were performed on two batches of samples.

III. RESULTS AND ANALYSIS

The resistivity of $(Ce_{1-x}La_x)_3Al$ alloys for $0\leqslant x\leqslant 1$ as a function of temperature is shown in Fig. 2. The hysteretic structural transition which occurs near $T_s=110$ K for Ce_3Al gives rise to a nonmonotonic feature in the resistivity. The transition temperature T_s decreases rapidly on alloying, and is not visible for $x=0.5-0.7$; but a similar feature in the resistivity is observed for $x=0.82-1.0$. Low-temperature x-ray diffraction on polished and powdered samples of Ce_3Al exhibited a profile consistent with that expected for the monoclinic phase.[4] The high multiplicity lines of the Ni_3Sn structure are split in the monoclinic structure; given the resolution and signal-to-noise of the present diffraction experiment, this splitting results in a marked broadening of the x-ray lines and changes in the relative line intensities,

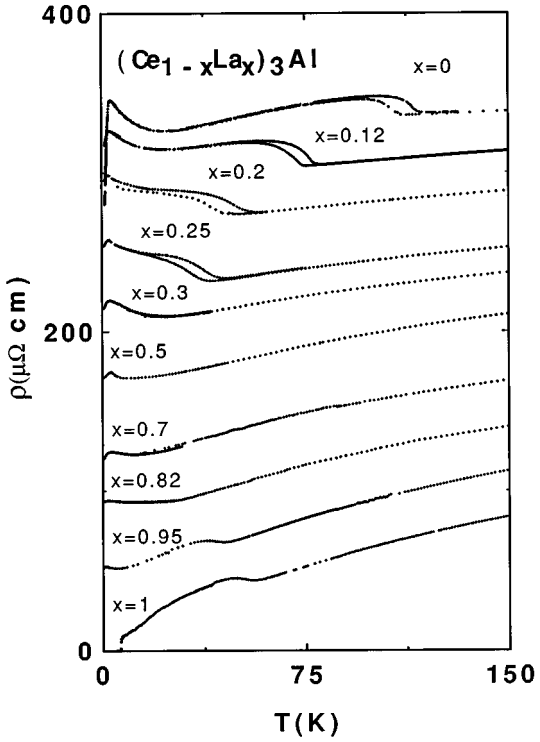

FIG. 2. The resistivity of $(Ce_{1-x}La_x)_3Al$ for various values of x as a function of temperature for $T<150$ K. Successive curves for decreasing alloy parameter x are offset by a constant amount, 25 $\mu\Omega$ cm. The hysteresis seen for $x=0-0.3$ arises from the first-order structural phase transition at $T=T_s$. The temperatures $T_{\max}(\rho)$ of the resistance maxima near 2 K, $T_{\min}$ of the resistance minima near 20 K and T_s are given in Table I.

consistent with a profile calculated assuming the parameters of Ref. 4. For La_3Al, however, the low-temperature profile was identical, within the resolution, to that observed at room temperature. This suggests that either the low-temperature phase of La_3Al also has the Ni_3Sn structure, or that the changes in the profile are too subtle to be resolved by ordinary x-ray diffraction. Since an isostructural phase transition seems inconsistent with the observed resistance anomaly (Fig. 2) we believe that the latter is the case. We plot the temperatures T_s in Fig. 3, with a question mark for the low-temperature phase of La_3Al.

For all the alloys with $x<1$, the low-temperature resistivity decreases with increasing temperature over an appreciable interval. This suggests the existence of the Kondo effect, for which the high-temperature contribution to the resistivity should vary[10] as

$$\rho_K(T)\propto -|JN(\epsilon_F)|^3\ln(kT/\epsilon_F) \tag{1}$$

where J is the Kondo exchange parameter, and ϵ_F is the Fermi energy. In Fig. 4 we plot the magnetic resistivity $\rho_m(T)=\rho[(Ce_{1-x}La_x)_3Al]-\rho(La_3Al)$ versus the logarithm of the temperature. [La_3Al experiences a structural transition at 50 K and a superconducting transition at 6 K. The values of $\rho(La_3Al)$ used for the determination of ρ_m have been extrapolated below T_c and smoothed in the vicinity of T_s.] The slope $d\rho/d(\ln(T))$ is seen to be nearly identical for all alloy concentrations $x\leqslant 0.3$, which suggests that J, and hence the

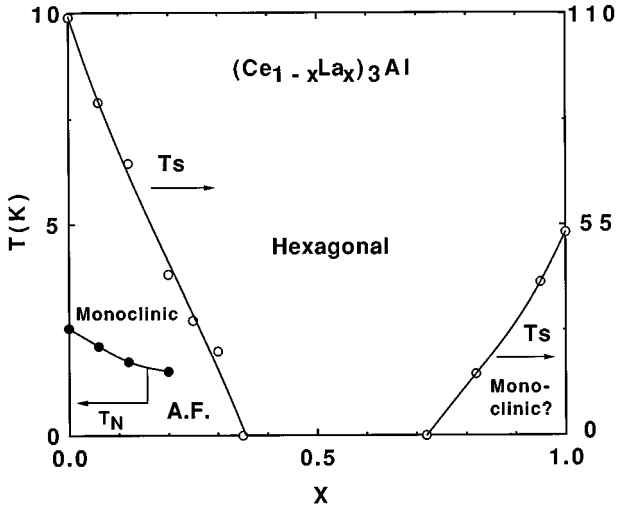

FIG. 3. The phase diagram of $(Ce_{1-x}La_x)_3Al$ for different x. The solid circles represent the Néel temperatures T_N; the open circles represent the structural transition temperatures T_s (taken as the midpoint of the hysteresis loop). The low-temperature phase for La_3Al is an open question.

Kondo temperature ($T_K \sim \exp[-1/JN(\epsilon_F)]$), is constant for these concentrations. Associated with the negative $d\rho/dT$ is a resistance minimum. From Fig. 2 and Table I it can be seen that the temperature $T_{\min}$ of this minimum is also constant ($T_{\min} \approx 23$ K) for $0 \leq x \leq 0.3$; since $T_{\min}$ is often taken as an estimate of the Kondo temperature (it is actually an upper limit) this also suggests that T_K is constant for $x \leq 0.3$. For

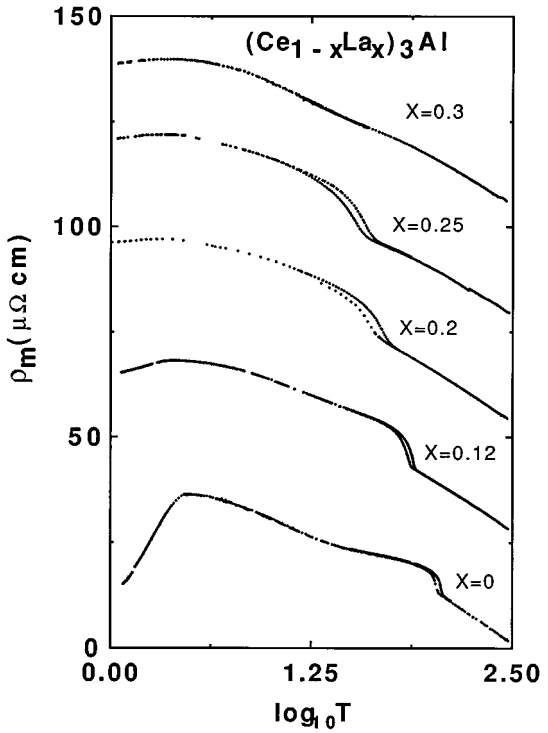

FIG. 4. The magnetic resistivity $\rho_m(T)$ vs $\ln(T)$, where $\rho_m = \{\rho[(Ce_{1-x}La_x)_3Al] - \rho[La_3Al]\}/3(1-x)$ is normalized to the number of Ce atoms. Successive curves for increasing alloy parameter x are offset by an amount 25 $\mu\Omega$ cm.

TABLE I. The average temperatures T_s of the α-γ structural phase transitions, with the limits of hysteresis in parentheses; the temperature $T_{\max}(\rho)$ of the resistivity maximum, and the temperature $T_{\min}$ of the resistivity minimum for different alloy concentrations x in $(Ce_{1-x}La_x)_3Al$.

x	T_s (K)	$T_{\max}(\rho)$ (K)	$T_{\min}$ (K)
0	110 (100,120)	3.2	23
0.06	87 (77,97)	2.9	23
0.12	71 (62,80)	2.5	22
0.2	42 (32,55)	2.4	≈17
0.25	30 (15,45)	2.8	≈15
0.3	22 (15,32)	3.0	≈23
0.5		3.3	18
0.7		3.2	12
0.82	16 (7,25)	2.6	≈12
0.95	40 (36,45)	1.0	5.5
1.0	52 (51,56)		

larger x both the slope of the resistivity and $T_{\min}$ decrease, suggesting that T_K decreases for these x.

The resistivity has a *maximum* at a temperature $T_{\max}(\rho) \approx 2$–3 K for all $x < 1$. For small x this arises from the onset of magnetic order; the maximum occurs at a temperature slightly higher than the Néel temperature T_N, since critical fluctuations decrease the scattering even for $T > T_N$. For larger x, the maximum may represent the onset of coherence in the Ce lattice, as discussed below. The values of $T_{\min}$, $T_{\max}(\rho)$, and T_s, are given for the different x in Table I.

The susceptibility $\chi(T)$ for several alloys is shown in Fig. 5. At high temperatures χ follows a Curie-Weiss law, $\chi(T) = C/(T+\theta_h)$ where the Curie constants are taken as equal that of a free $J = 5/2$ Ce ion ($C = 0.807$ emu/mole K) and the Weiss temperature θ_h (Table II) is positive. A positive Weiss temperature reflects demagnetization which can arise from crystal-field effects, the Kondo effect, or antiferromagnetic fluctuations; it can be phenomenologically represented by the formula $\theta_h = aT_N + bT_K + cT_{cf}$ where T_{cf} is the crystal-field splitting and a, b, and c are of order unity. We will show below that the Kondo temperatures (5–10 K) and Néel temperatures (<2.5 K) are nearly an order of magnitude smaller than the Weiss temperatures (55–80 K); hence the probable origin of the latter is the crystal-field effect. We note that θ_h decreases with x, suggesting that the crystal-field splitting decreases with increasing x.

The low-temperature susceptibility also follows a Curie-Weiss law $C_1/(T+\theta_1)$; where $C_1 \approx 0.4$ emu/mole Ce K and $\theta_1 \approx 10$ K for $0 \leq x \leq 0.3$, but for larger x, C_1 increases somewhat and θ_1 decreases substantially (Table II). For these temperatures, the susceptibility arises from the lowest crystal-field doublet; the constancy of C_1 for $0 \leq x \leq 0.3$ means that the wave function for the doublet, and hence the moment, does not change, even though the splitting does change. Since $T_N \approx 2$ K $< \theta_1$, the Weiss parameter here measures $T_K \approx 10$ K for $0 \leq x \leq 0.3$. (This is only an approximation, because as we discuss below, the cerium atoms on different inequivalent sites in the monoclinic structure can, in principle, have different Kondo temperatures.) The smaller θ_1 at

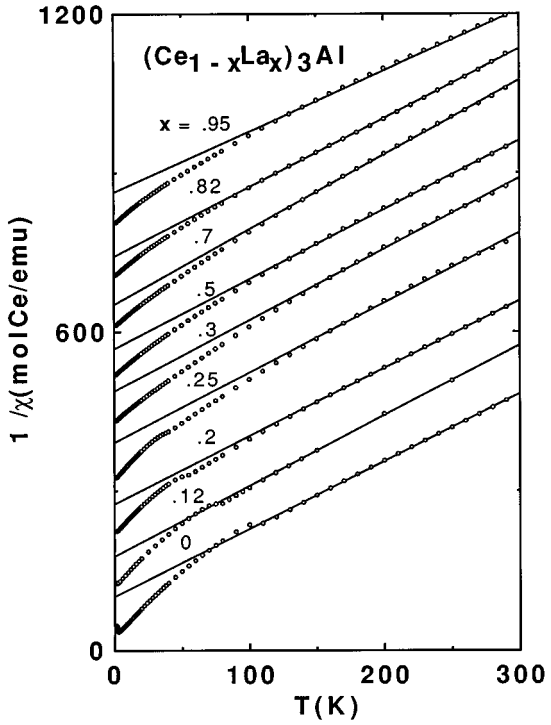

FIG. 5. The susceptibility, plotted as $1/\chi$ versus the temperature. Successive curves for increasing x are offset by the constant amount 100 mole Ce/emu. The solid lines represent fits to the Curie-Weiss form at high temperature; the parameters of the fits are given in Table II.

larger x then would reflect a decreasing T_K. These conclusions are consistent with those drawn earlier from the resistivity.

The low-temperature susceptibility is shown in Fig. 6. A peak, due to the onset of antiferromagnetic order, is observed at $T_{\max}(\chi)\approx 3$ K for $x=0$; this temperature (Table II) decreases with decreasing x until for $x\geq 0.2$ it is no longer visible for the temperature range ($T>1.8$ K) of our experiment. As for the resistivity, the susceptibility is decreased

TABLE II. The high- (200–300 K) temperature Weiss parameter θ_h and low- (3–10 K) temperature Curie constant C_1 and Weiss temperature θ_1 for the susceptibility $\chi(T)$ for different alloy concentrations x of $(Ce_{1-x}La_x)_3Al$. $T_{\max}(\chi)$ is the temperature of the low-temperature maximum, indicating the onset of antiferromagnetism.

x	θ_h (K)	C_1 (emu K/mol Ce)	θ_1 (K)	$T_{\max}(\chi)$ (K)
0	82	0.39	10	2.9
0.06	75	0.38	8	2.5
0.12	68	0.39	8	2.1
0.2	64	0.39	7.8	
0.25	68	0.38	7.7	
0.3	60	0.43	11	
0.5	52	0.45	7.5	
0.7	50	0.45	3.6	
0.82	40	0.47	1.9	
0.95	37	0.45	0.7	

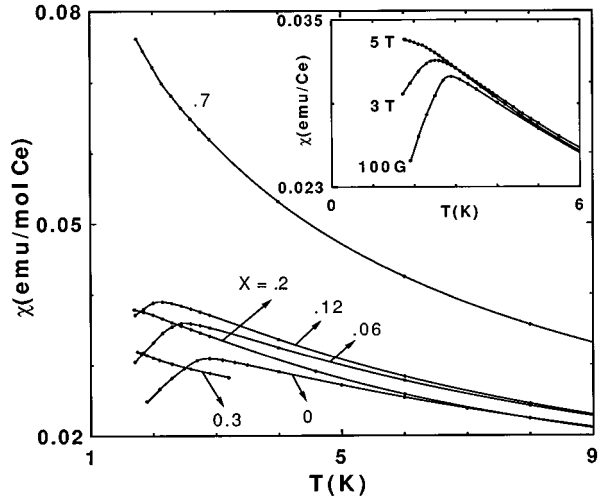

FIG. 6. The low-temperature magnetic susceptibility $\chi(T)$ versus temperature. The maxima indicate the onset of antiferromagnetism. The inset shows the magnetic-field dependence of the susceptibility of Ce_3Al.

above T_N due to critical fluctuations, and hence $T_{\max}(\chi)>T_N$. The data confirms the trend observed for $T_{\max}(\rho)$: T_N initially decreases with x. The data of Fig. 6 also give a second way to estimate T_K, by using the Bethe-ansatz formula $T_K=C_L/\chi(0)$.[8] For $0\leq x\leq 0.3$ the largest observed values of χ vary from 0.03–0.04 emu/mole Ce; using these values to estimate $\chi(0)$ we arrive at the conclusion that T_K is approximately constant at 10–13 K for $0\leq x\leq 0.3$ and then reduces to 6 K for $x=0.7$. We note that these values of T_K are consistent with those given above.

The specific heat per formula unit is shown in Fig. 7. Sharp peaks in $C(T)$ occur for $x<0.3$ due to the antiferromagnetic order; the temperature of the maximum is the best measure of the Néel temperature. For larger x the peaks are broad, reflecting both the Kondo effect and the onset of coherence (i.e., magnetic correlations), as discussed below. The Néel temperatures T_N and the temperature $T_{\max}(C)$ of the maxima for larger x are given in Table III; $T_N(x)$ is plotted in Fig. 3. We note that $T_{\max}(C)<T_{\max}(\chi)<T_{\max}(\rho)$; the difference between the successive temperatures is of order 0.3 K. As discussed above, the difference arises from the effect of critical fluctuations on the resistivity and susceptibility.

In order to analyze this data, we must account for contributions to the specific heat from phonons, crystal fields (which for the low crystal symmetry should split the $J=5/2$ line into three doublets), Kondo demagnetization, and magnetic correlations. For $x=0$, we assume a constant Debye temperature $\theta_D=210$ K to generate the phonon contribution $C_{\rm ph}(T)$; we subtract this from the data to obtain the magnetic specific heat $C_m(T)=C(T)-C_{\rm ph}(T)$ [Fig. 8(a)]. The crystal-field contribution $C_{\rm cf}(T)$ plotted in Fig. 8(a) is that of a Schottky contribution from the doublets with crystal-field splittings $T_{1\rm cf}=75$ K and $T_{2\rm cf}=130$ K. (These values for θ_D, $T_{1\rm cf}$, and $T_{2\rm cf}$ are similar to the values 215, 65, and 130 K, respectively, used in Ref. 5). The remaining specific heat yields an integrated entropy of $R\ln 2$ as expected for a ground-state doublet. This remainder reflects both the contribution from the magnetic phase transition and that due to heavy-fermion demagnetization. Since the theoretical func-

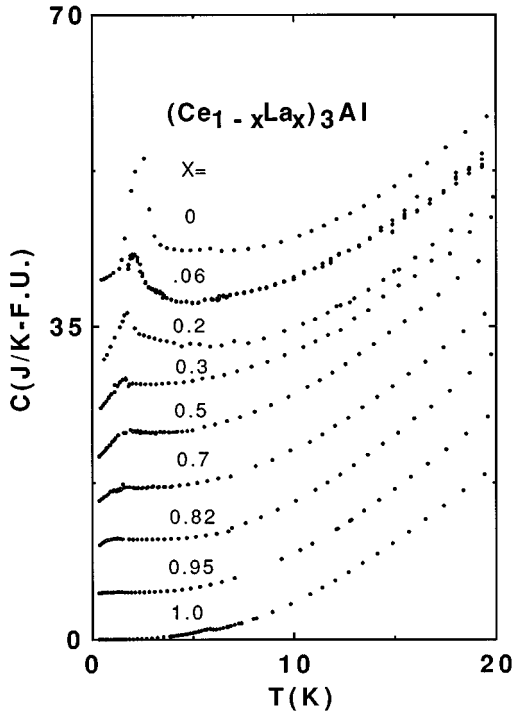

FIG. 7. The specific heat per formula unit for $(Ce_{1-x}La_x)_3Al$ versus temperature at low temperature. Successive curves for decreasing x are offset by the constant amount 5 J/K f.u.

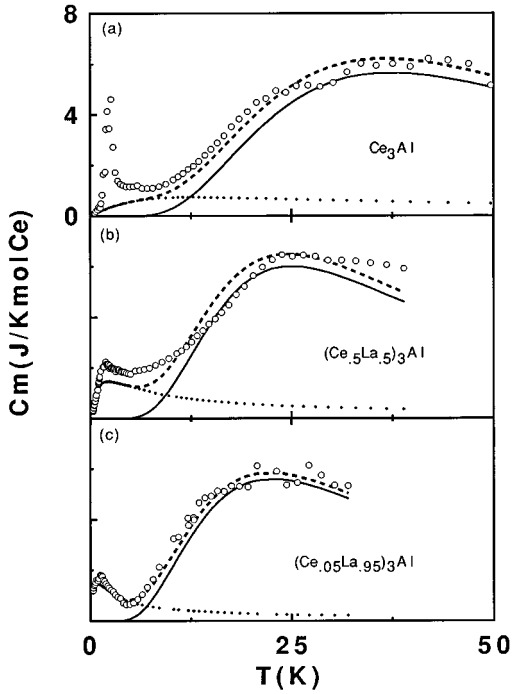

FIG. 8. The magnetic specific heat per mole Ce, $C_m(T)=C(T)-C_{ph}(T)$ (open circles) of $(Ce_{1-x}La_x)_3Al$ for (a) $x=0$, (b) $x=0.5$, and (c) $x=0.95$, where C_{ph} is the phonon contribution (see text). The dashed line is the prediction for $C_m(T)$ which is the sum of a Schottky anomaly $C_{cf}(T)$ (solid line) and a Kondo impurity contribution (Ref. 8) $C_K(T)$ (dotted line) with crystal-field splittings and Kondo temperatures as given in Table III. The Kondo impurity theory works very well for large x. For small x, $C_m(T)$ is dominated by the anomaly due to the antiferromagnetic phase transition for $0<T<5$ K; to fit the data for $T>10$ K, we assume a Kondo contribution from 50% of the sites. For intermediate x (e.g., $x=0.5$) the low-temperature peak in C_m is somewhat sharper than for a Kondo impurity, suggesting that magnetic correlations persist, even in the nonmagnetic ground state.

tional form for the specific heat under these circumstances is unknown, we adopt an *ad hoc* procedure. In the monoclinic structure there are six inequivalent cerium sites;[4] we assume that only half (three) of these sites undergo magnetic order and the other three give a Kondo contribution. Using the Bethe-ansatz results[11] to estimate the Kondo contribution $C_K(T)$ we get good agreement for $T>10$ K for choices of $T_K\approx 10$ K; at lower temperature, the large specific-heat maximum would then be associated with magnetic ordering on the other half of the sites. For $x=0.2$, a similar procedure (with $\theta_D=195$ K but with smaller crystal-field splitting, see Table III) gives similar results. In the opposite limit of large alloy parameter ($x=0.95$), we use the specific heat of La_3Al to estimate $C_{ph}(T)$. The data can be fit fairly well [Fig. 8(c)] assuming crystal-field splittings $T_{1cf}=45$ K, $T_{2cf}=80$ K and a Kondo contribution $C_K(T)$ from all (100%) of the sites with

TABLE III. The temperature $T_{max}(C)$ of the maximum of $C(T)$ (for $x\leqslant 0.2$ this is the Néel temperature T_N); the Kondo temperature T_K(fit) (for $0\leqslant x\leqslant 0.3$, the Kondo contribution is assumed to arise from only half the cerium sites), the temperatures of the low-lying crystal-field T_{1cf} and the high-lying crystal-field T_{2cf} used in the fits (Fig. 8) to the low-temperature specific heat; and the $T\rightarrow 0$ value $\gamma(0)$ of the linear coefficient of specific heat (Fig. 9) and Kondo temperature estimated using $T_K(\gamma)=\pi R/6\gamma(0)$ (Ref. 8).

x	$T_{max}(C)$ (K)	T_K(fit) (K)	T_{1cf} (K)	T_{2cf} (K)	$\gamma(0)$ (J/mole Ce K^2)	$T_K(\gamma)$ (K)
0	2.54	15 (50%)	75	130	0.2	22
0.06	2.12					
0.12	1.75					
0.2	1.52	12 (50%)	60	110	0.7	6.2
0.3	1.7	3 (50%)	55	80	0.9	4.8
0.5	1.7	2.7 (100%)	55	80	1.0	4.3
0.7	1.7	2.7 (100%)	50	80	1.5	2.9
0.82	1.85	1.6 (100%)	50	80	3.0	1.5
0.95	1.75	1.0 (100%)	45	80	3.6	1.2

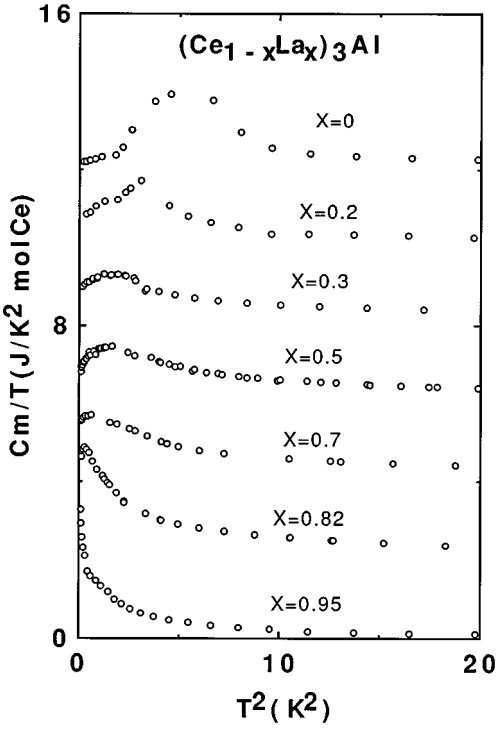

FIG. 9. The magnetic specific heat (per mole Ce) plotted versus the square of the temperature. Successive curves for decreasing values of alloy parameter x are offset by the constant amount 2 J/mole Ce K^2. The specific heat is linear as $T\rightarrow 0$, even in the antiferromagnetic state for small x. The low-temperature linear coefficients $\gamma(0)$ are given in Table III.

a small value for the Kondo temperature $T_K=1$ K. For $x=0.5$, 0.7, and 0.82, we assume a phonon contribution $C_{\rm ph}(T)$ similar to that of La_3Al, with crystal-field splittings of order $T_{1cf}\approx 50$ K and $T_{2cf}=80$ K and Kondo temperatures of order 2 K. We obtain qualitative agreement with the data [Fig. 8(b)], but the theory underestimates the data at low temperature (1–5 K) and overestimates the data for $10<T<20$ K.

While such an analysis is not unique, we emphasize that there are several constraints on the procedure. The phonon contributions are reasonable; and after subtraction of the phonon and Schottky contribution, the remaining specific heat gives the expected $R\ln 2$ integrated entropy. For small x the procedure is admittedly *ad hoc*, but nevertheless the fraction of sites making a Kondo contribution is chosen to give the correct magnitude of total specific heat for $T>10$ K. For $x=0$ and 0.2, the fits for $T>10$ K are not very sensitive to the value chosen (12–15 K) for the Kondo temperature; however, for significantly smaller T_K (e.g., 1 K) the theory underestimates the specific heat at high temperature. Finally, the values for the crystal-field splittings and Kondo temperatures are similar to those deduced from the susceptibility using the Weiss parameters; in particular $T_K(\text{fit})\approx\theta_l$ and $T_{1cf}\approx\theta_h$. Hence, while the parameters given in Table III have substantial uncertainty, they correctly reflect the trends in the magnitudes of the crystal-field splittings and Kondo temperatures with increasing x.

In Fig. 9 we plot the quantity $C_m(T)/T$ versus T^2 for several concentrations. The $T\rightarrow 0$ linear coefficients $\gamma(0)$ deduced from this plot are given in Table III, as well as the single impurity Kondo temperature deduced from the Bethe-ansatz result $T_K(\gamma)=\pi R/6\gamma(0)$,[8] where R is the gas constant. We note that the resulting estimates for the Kondo temperature qualitatively agree with those used in the fits to C_m (Fig. 8). The $T\rightarrow 0$ specific heat is linear even in the antiferromagnetic state for small x, with $\gamma(0)\approx 0.2$, 0.7, and 0.9 J/mole Ce K^2 for $x=0$, 0.2, and 0.3, respectively. The existence of a large linear coefficient of specific heat below T_N potentially means that heavy-fermion processes (which give a linear behavior) may persist in the antiferromagnetically ordered ground state.

IV. DISCUSSION

In agreement with older work,[6,7] our data shows that the temperature of the structural transition to the monoclinic phase of Ce_3Al decreases rapidly upon alloying with La. In addition, we show that for $x=1$ (La_3Al), 0.95, and 0.82 a phase transition with a similar feature in the resistivity occurs. The low-temperature phase for these x is not monoclinic, however, and the diffraction profiles are similar to those for the hexagonal (Ni_3Sn) phase. The structure of the ground state of La_3Al is an open question.

In Ce_3Al the temperature T_s initially increases on application of pressure at a rate $\Delta T_s/\Delta P\approx 2.5$ K/kbar;[1] it decreases on alloying with La at a rate $\Delta T_s/\Delta x\approx 3.1$ K/at. % (Fig. 3). The room-temperature cell volume simultaneously increases (Fig. 1) at a rate $\Delta V/V_0\Delta x\approx 8.7\times 10^{-4}$/at. % due to the larger size of the La ion relative Ce. These numbers can be compared by estimating the bulk modulus from the formula

$$B=(\Delta T_s/\Delta x)/[(\Delta T_s/\Delta P)(\Delta V/V_0\Delta x)]\approx 1400 \text{ kbar}.$$

This is somewhat larger than expected, which could reflect the fact that the alloy disorder causes $\Delta T_s/\Delta x$ to be larger than it would be based on chemical pressure alone; i.e., the monoclinic phase is destabilized by alloy disorder as well as by negative pressure. This is consistent with the observation[6] that alloying with either La or Y leads to a suppression of T_s, even though the chemical pressures exerted by these solutes have the opposite sign.

An interesting feature of the structural transition is that at $x=0$, $T_{cf}\approx T_s$ and the decrease in T_s appears to correlate with the initial decrease in the crystal-field splittings, as determined from the fits to the specific heat (Table III), or from the Weiss parameter $\theta_h(x)$ (Table II). This suggests that the transition to the monoclinic phase occurs when the crystal fields becomes depopulated; as the splitting decreases, the transition occurs at a lower temperature.

The increase in cell volume on alloying with La is also expected to change the Kondo temperature; since La is larger than Ce the negative chemical pressure should decrease the $4f$/conduction electron hybridization and cause the Kondo coupling J, and hence T_K, to decrease with increasing x. Over the whole range of x, this is clearly true: the Weiss parameter θ_1 (Table II), the low-temperature susceptibility (Fig. 6), the fits to C_m (Fig. 8 and Table III) and the values of $\gamma(0)$ (Fig. 9 and Table III) all indicate that T_K decreases from ≈ 10 K for small x to ≈ 1 K for large x.

The sharp peaks in the specific heat for $x=0$ and 0.2 clearly indicate the onset of antiferromagnetic order. For

larger x the peaks are much broader. For $x=0.95$ the peak in $C(T)$ can be fit assuming it arises from the Kondo effect, with no contribution from magnetic order; for $x=0.5-0.82$ the peak in $C(T)$ has greater magnitude and is sharper than expected for the Kondo effect alone but is much broader and smaller (2 J/mole Ce K) than for the case of magnetic order. These facts suggest that the maxima in $C(T)$ and $\rho(T)$ which occur near 1–2 K for $x=0.5-0.95$ are not associated with magnetic order but instead reflect both the Kondo effect (entirely dominant for $x=0.95$) and the magnetic correlations which are expected even in the nonmagnetic heavy fermion ground state; i.e., they represent the onset of ''coherence'' in the Ce lattice. The correlations cause the low-temperature specific-heat peak to be sharper, and of greater magnitude, than if the Kondo effect alone were operative, and cause a decrease in resistivity for $T<T_{\max}(\rho)$.

Finally, we discuss whether magnetic order and heavy-fermion behavior coexist below T_N for $0\leqslant x<0.3$. The evidence for this is as follows. First, at temperatures just larger than T_N, the resistivity shows a negative slope and the susceptibility shows demagnetization effects (Weiss parameter θ_1 of order 10 K; reduced value of susceptibility at T_N) which indicate that the magnetic order occurs at a temperature where the Kondo effect is strong. Second, the linear coefficient of specific heat has a large value ($\gamma(0)\approx 0.2-0.9$ J/mole Ce K^2) for $x=0-0.3$ even below T_N which can be taken as indicating that heavy-fermion behavior persists in the magnetically ordered state. Given the monoclinic symmetry of γ-Ce_3Al, one way this might happen is that the magnetic order may only occur on a fraction of the six inequivalent Ce sites, while the remaining sites could be nonmagnetic due to the heavy-fermion processes. This is part of the motivation for the manner in which we have fit the specific heat for small x.

V. CONCLUSION

This work raises several issues concerning the alloy system $(Ce_{1-x}La_x)_3Al$: the structure of the ground state of La_3Al; whether the decrease of the structural transition temperature T_s on alloying correlates with a decrease in crystal-field splittings; whether the ground state for $0.3\leqslant x\leqslant 0.7$ is magnetically ordered, or is a nonmagnetic heavy-fermion state with appreciable magnetic correlations; whether heavy-fermion behavior coexists with antiferromagnetic order below T_N in the ground state for $0\leqslant x\leqslant 0.3$, and if so, whether Ce atoms on only a fraction of the six inequivalent sites in the monoclinic structure undergo order, while the remainder are nonmagnetic due to the Kondo effect. These questions can be answered by a combination of neutron diffraction, to determine the structure of La_3Al at low temperature and the magnetic order in Ce_3Al and its alloys for small x, and inelastic neutron scattering to determine the crystal-field splittings and the spin dynamics and thus show directly whether spin fluctuations exist in the ordered phase. Preliminary studies of the magnetic structure of Ce_3Al are underway.[12]

ACKNOWLEDGMENTS

This work was supported by the National Council of the Republic of China under Grants No. NSC84-2112-M-001-033 and NSC85-2112-M-008-027.

[1] Y. Y. Chen, J. M. Lawrence, J. D. Thompson, and J. O. Willis, Phys. Rev. B **40**, 10 766 (1989).
[2] M. Sera, T. Satoh, and T. Kasuya, J. Magn. Magn. Mater. **63&64**, 82 (1987).
[3] J. Sakurai, T. Matsuura, and Y. Komura, J. Phys. (Paris) Colloq. **49**, C8-783 (1988).
[4] A. C. Lawson, J. M. Lawrence, J. D. Thompson, and A. Williams, Physica B **163**, 587 (1990).
[5] S. Y. Wu, W. T. Hsieh, W.-H. Li, K. C. Lee, and Y.-Y. Chen, Chin. J. Phys. **31**, 663 (1993).
[6] J. Sakurai, Y. Murashita, Y. Aoki, T. Fujita, T. Takabatake, and H. Fujii, J. Phys. Soc. Jpn. **58**, 4078 (1989).
[7] C. S. Garde, J. Ray, and G. Chandra, J. Phys. Condens. Matter **1**, 2737 (1989).
[8] T. Suzuki, Y. Aoki, S. Nishigori, T. Fujita, Y. Murashita, and J. Sakurai, J. Magn. Magn. Mater. **90&91**, 482 (1990).
[9] Y. Y. Chen, Y. D. Yao, B. T. Lin, S. G. Shyu, and H. M. Lin, Chin. J. Phys. **32**, 479 (1994).
[10] G. Oomi, T. Numata, and J. Sakurai, Physica B **149**, 73 (1988).
[11] V. T. Rajan, Phys. Rev. Lett. **51**, 309 (1983).
[12] W. H. Li (unpublished).